Design of a highly potent HIV-1 fusion inhibitor targeting the gp41 pocket

Huihui Chong, Zonglin Qiu, Yang Su, Lingli Yang and Yuxian He

Objective: T20 (Enfuvirtide), which is a 36-residue peptide derived from the C-terminal heptad repeat (CHR) of gp41, is the only clinically available HIV-1 fusion inhibitor, but it easily induces drug resistance, which calls for next-generation drugs.

Design: We recently demonstrated that the M-T hook structure can be used to design a short CHR peptide that specifically targets the conserved gp41 pocket rather than the T20-resistant sites. We attempted to develop more potent HIV-1 fusion inhibitors based on the structure–activity relationship of MT-SC22EK.

Methods: Multiple biophysical and functional approaches were performed to determine the structural features, binding affinities and anti-HIV activities of the inhibitors.

Results: The 23-residue peptide HP23, which mainly contains the M-T hook structure and pocket-binding sequence, showed a helical and trimeric state in solution. HP23 had dramatically improved binding stability and antiviral activity, and it was the most potent inhibitor of the M-T hook-modified and unmodified control peptides. More promisingly, HP23 was highly active in the inhibition of diverse HIV-1 subtypes, including T20 and MT-SC22EK resistant HIV-1 mutants, and it exhibited a high genetic barrier to the development of resistance.

Conclusion: Our studies delivered an ideal HIV-1 fusion inhibitor that specifically targeted the highly conserved gp41 pocket and possessed potent binding and antiviral activity. Furthermore, HP23 can serve as a critical tool to explore the mechanisms of HIV-1 fusion and inhibition.

AIDS 2015, **29**:13–21

Keywords: drug resistance, fusion inhibitor, genetic barrier, HIV-1, M-T hook structure

Introduction

HIV-1 infection requires fusion between viral and cellular membranes, which is initiated by attachment of the viral envelope (Env) glycoprotein to cells [1,2]. In the current model, binding of the surface gp120 to the CD4 receptor and a coreceptor (CCR5 or CXCR4) induces large conformational changes in the gp120/gp41 complex, which activates the fusion machinery of the transmembrane gp41 subunit (Fig. 1). Briefly, the N-terminal fusion peptide of gp41 is inserted into the cell membrane to mediate a prehairpin intermediate state. Next, three C-terminal heptad repeats (CHRs) fold antiparallelly onto the trimeric coiled coil of the N-terminal heptad repeats (NHRs), which results in a stable six-helix bundle (6-HB) to bridge the viral and cellular membranes into close proximity [3–5]. The crystal structure of 6-HB identified a deep pocket on the C-terminal portion of NHR helices, which is penetrated by three hydrophobic residues from the pocket-binding domain (PBD) of the CHR helix [3–6]. It is evident that the pocket region critically determines the stability of the 6-HB core and the fusogenic activity of gp41, which offers an ideal target site for anti-HIV agents [6–8].

T20 (Enfuvirtide), which is a 36-residue peptide derived from the native CHR sequence, is the only HIV-1 fusion inhibitor approved for clinical use, but it easily induces

MOH Key Laboratory of Systems Biology of Pathogens and AIDS Research Center, Institute of Pathogen Biology, Chinese Academy of Medical Sciences & Peking Union Medical College, Beijing, P. R. China.

Correspondence to Yuxian He, MD, Institute of Pathogen Biology, Chinese Academy of Medical Sciences, 9 Dongdan Santiao, Beijing 100730, China.

Tel: +8610 67870275; fax: +8610 67873372; e-mail: yhe@ipb.pumc.edu.cn
Received: 7 July 2014; revised: 16 September 2014; accepted: 23 September 2014.

DOI:10.1097/QAD.0000000000000498

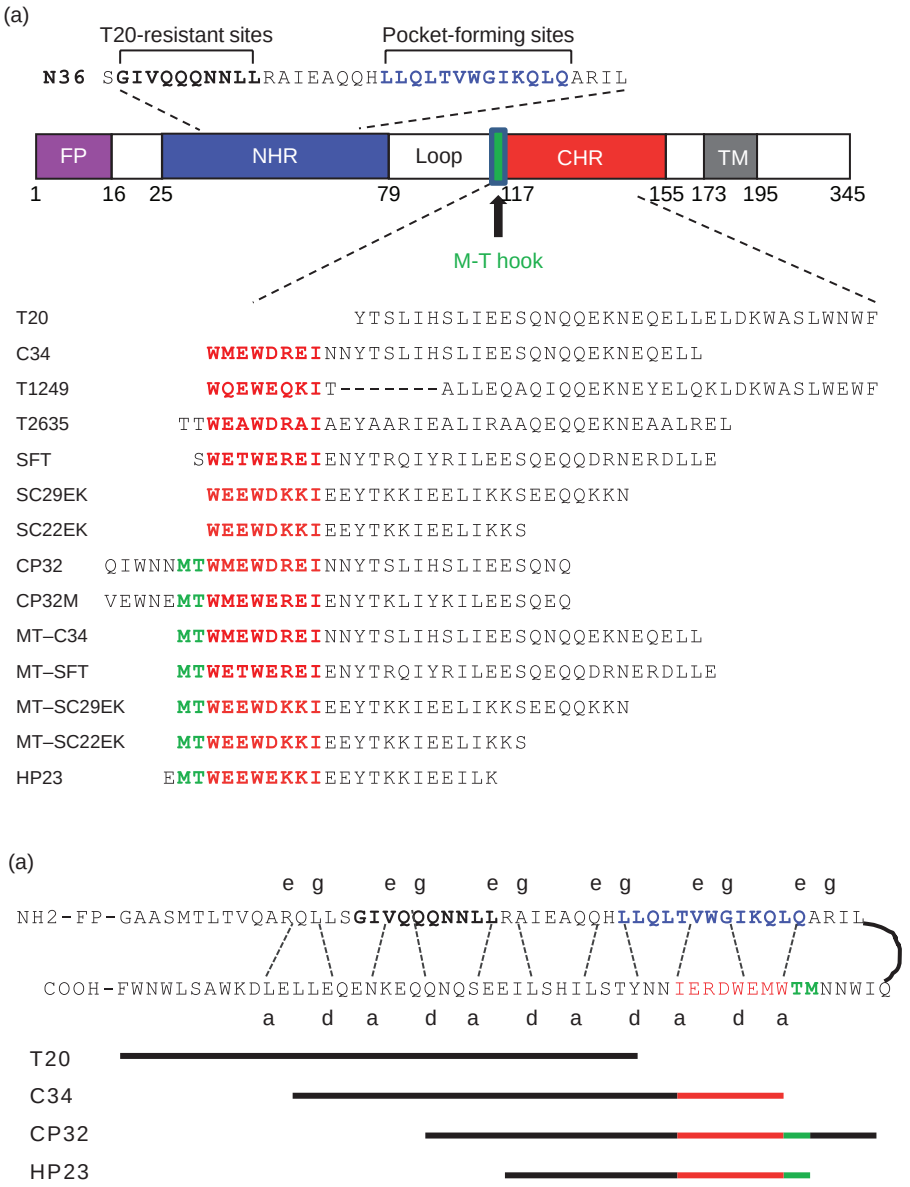

Fig. 1. Schematic illustration of HIV-1 gp41 protein and its peptide inhibitors. (a) The functional domains of gp41 and the sequences of NHR or CHR-derived peptides. The gp41 numbering of HIV-1_{HXB2} is used. The sequences corresponding to the NHR pocket region are marked in blue, and sequences corresponding to the CHR pocket-binding domain (PBD) are marked in red. The position and sequence of the M-T hook structure are marked in green. (b) The interaction between the NHR and CHR of gp41. The dashed lines between the NHR and CHR regions indicate the interaction between the residues located at the *e*, *g* and *a*, *d* positions in the NHR and CHR, respectively. The peptide inhibitors are positioned as lines to express their sequence and binding sites. CHR, C-terminal heptad repeat; FP, fusion peptide; NHR, N-terminal heptad repeat; TM, transmembrane domain.

drug-resistance both *in vitro* and *in vivo* [9–12]. The mutations responsible for T20-resistance are largely mapped to the inhibitor-binding sites on the NHR of gp41 (Fig. 1). The CHR peptide C34 (34-residue) has been widely used as a template for peptide engineering because of the lack of pocket-binding residues by T20, which resulted in several inhibitors with significantly improved pharmaceutical profiles, such as Sifuvirtide (SFT, 36-residue) [13], SC35EK (35-residue) [14] and T2635 (TRI-1144, 38-residue) [15]. SFT has been approved for clinical Phase III trials in China and will hopefully become the second HIV-1 fusion inhibitor in clinical use. Unfortunately, SFT has a relatively low genetic barrier to the development of drug resistance during in-vitro selection, and the resulting HIV-1 variants display high cross-resistance to T20 [13,16]. Therefore, new strategies or concepts are required to develop next-generation drugs that block HIV-1 fusion. We recently demonstrated that two residues (Met115 and Thr116) preceding the PBD of CHR peptides adopt a

unique M-T hook structure that greatly enhance the pocket-binding and antiviral activities [17,18], which provides a totally new strategy to design or optimize HIV-1 fusion inhibitors. Promisingly, we successfully generated the short peptide MT-SC22EK (24-residue), which primarily contains the M-T hook structure and PBD sequence, to target the deep pocket rather than the T20 and SFT-resistant sites [19]. In this study, we designed a 23-residue helical, trimeric peptide named HP23 on the basis of the structure–activity relationship (SAR) of MT-SC22EK. HP23 exhibited the highest binding stability and the most potent anti-HIV activity compared with both the template and a large panel of control peptides. More importantly, HP23 showed a dramatically improved potency in the inhibition of T20 and MT-SC22EK resistant HIV-1 mutants and a high genetic barrier to the development of resistance.

Materials and methods

Peptide synthesis

Peptides were synthesized using a standard solid-phase 9-flurorenylmethoxycarbonyl (FMOC) method as described previously [18]. All peptides were acetylated at the N-terminus and amidated at the C-terminus. Peptide concentrations were determined using ultraviolet (UV) absorbance and a theoretically calculated molar-extinction coefficient ε (280 nm) of 5500 and 1490 mol/l per cm. based on the number of tryptophan and tyrosine residues, respectively [20].

Circular dichroism spectroscopy

A CHR peptide was incubated with an equal molar concentration of N36 or its mutant at 37°C for 30 min in PBS (pH 7.2). Circular dichroism spectra were acquired on a Jasco spectropolarimeter (model J-815) using a 1-nm bandwidth with a 1-nm step resolution from 195 to 260 nm. The α-helical content was calculated from the circular dichroism signal by dividing the mean residue ellipticity [θ] at 222 nm by the value expected for 100% helix formation (−33 000° cm^2/dmol). Thermal denaturation was performed by monitoring the ellipticity change at 222 nm from 20°C to 98°C at a rate of 1.2°C/min as described previously [21].

Analytical ultracentrifugation

Sedimentation equilibrium experiments were performed using a Beckman Coulter ProteomeLab XL-I Protein Characterization System equipped with a standard two-channel cell in an An-60 Ti rotor, as described previously [22]. HP23 was diluted in 50 mmol/l KH_2PO_4/100 mmol/l KCl (pH 7.0) to final concentrations ranging from 9.3 to 600 μmol/l. Data were collected at 28 000 and 32 000 rpm at wavelengths of 280–300 nm (depending on peptide concentrations) at 4°C. Weight-averaged molecular weights were obtained by fitting each data file individually using a single ideal species model in the Beckman Origin software.

Isothermal titration calorimetry

Isothermal titration calorimetry (ITC) assays were performed using an ITC_{200} Microcalorimeter instrument (MicroCal, Northampton. Massachusetts, USA) as described previously [18]. Briefly, 1 mmol/l N36 peptide dissolved in ddH_2O was injected into a chamber containing 100 μmol/l MT-SC22EK or HP23. The experiments were performed at 25°C. The time between injections was 240 s, and the stirring speed was 500 rpm. Data acquisition and analysis were performed using the MicroCal Origin software (version 7.0).

Cell–cell fusion assay

A reporter gene assay based on the activation of an HIV long terminal region-driven luciferase cassette in TZM-bl cells (target) by HIV-1 tat from HL2/HL3 cells (effector) was described previously [19]. Briefly, TZM-bl cells were plated in 96-well plates (1×10^4/well) and incubated at 37°C overnight. Target cells were cocultured with HL2/HL3 cells (3×10^4/well) for 6 h at 37°C in the presence or absence of a test peptide at graded concentrations. Luciferase activity was measured using luciferase assay reagents and a luminescence counter (Promega, Madison, Wisconsin, USA).

Single-cycle infection assay

A single-cycle infection assay was performed as described previously [23]. Briefly, HIV-1 pseudovirus was generated via the cotransfection of 293T cells with an Env-expressing plasmid and a backbone plasmid $pSG3^{\Delta env}$ that encoded Env-defective, luciferase-expressing HIV-1 genome. Supernatants were harvested 48 h after transfection, and 50% tissue culture infectious dose ($TCID_{50}$) was determined in TZM-bl cells. Peptides were prepared in three-fold dilutions and mixed with 100 $TCID_{50}$ viruses. The mixture was added to TZM-bl cells (10^4/well), incubated for 48 h at 37°C and luciferase activity was measured.

Inhibition of HIV-1_{NL4-3} replication

Peptide inhibition of HIV-1 replication was determined using a molecular cloned wild-type HIV-1_{NL4-3}. Briefly, virus stock was harvested and quantified 48 h post-transfection. A total of 100 $TCID_{50}$ viruses were used to infect TZM-bl cells in the presence or absence of serially diluted peptides. Cells were harvested 2 days postinfection and lysed in reporter lysis buffer, and luciferase activity was measured.

Induction of HIV-1 resistance to inhibitors

The selection of HIV-1 resistance to inhibitors was performed as described previously [24]. Briefly, MT-4 cells were seeded at 1×10^4 in RPMI 1640 medium containing 10% foetal bovine serum in 12-well plates. The molecular clone of HIV-1_{NL4-3} was used to infect

cells in the presence or absence of diluted peptide inhibitors. Cells were incubated at 37°C with 5% CO_2 until an extensive cytopathic effect was observed. Culture supernatants were harvested and used for next passage on fresh MT-4 cells with 1.5 to two-fold increase in peptide concentrations.

Results

Design of a helical, oligomeric short-peptide inhibitor

We designed a novel peptide fusion inhibitor named HP23 on the basis of the structural and functional information of MT-SC22EK [19] (Fig. 1). In the designing rationale, two C-terminal residues (lysine and serine) of MT-SC22EK were deleted because they are not critical for binding, and three middle residues were changed to facilitate intra-helical and inter-helical interactions. A glutamic acid was added to the N-terminus of the peptide to stabilize M-T hook binding. The resulting peptide, HP23, had a 23-residue length and mainly targeted the pocket region on the NHR (Fig. 1b). Circular dichroism spectra of HP23 displayed typical double minima at 208 and 222 nm at different peptide concentrations (Fig. 2a), which indicated its α-helical feature. Its thermal unfolding transition (T_m) was dependent on the peptide concentration (Fig. 2b), which indicated a self-associating species. Therefore, we used analytical ultracentrifugation to examine association behaviour at several peptide concentrations. A radial scan for HP23 at a concentration of 150 μmol/l obtained a molecular mass of 9598 Da (Fig. 2c), which indicated that HP23 self-associated into a trimer status. Consistently, the HP23 trimer was observed over the peptide concentration range of 18–600 μmol/l (Fig. 2d).

HP23 binds to the N-terminal heptad repeat target with a high affinity

We previously demonstrated that the M-T hook structure modified MT-SC22EK binds to the NHR target with a high affinity [19]. Here, we investigated whether the

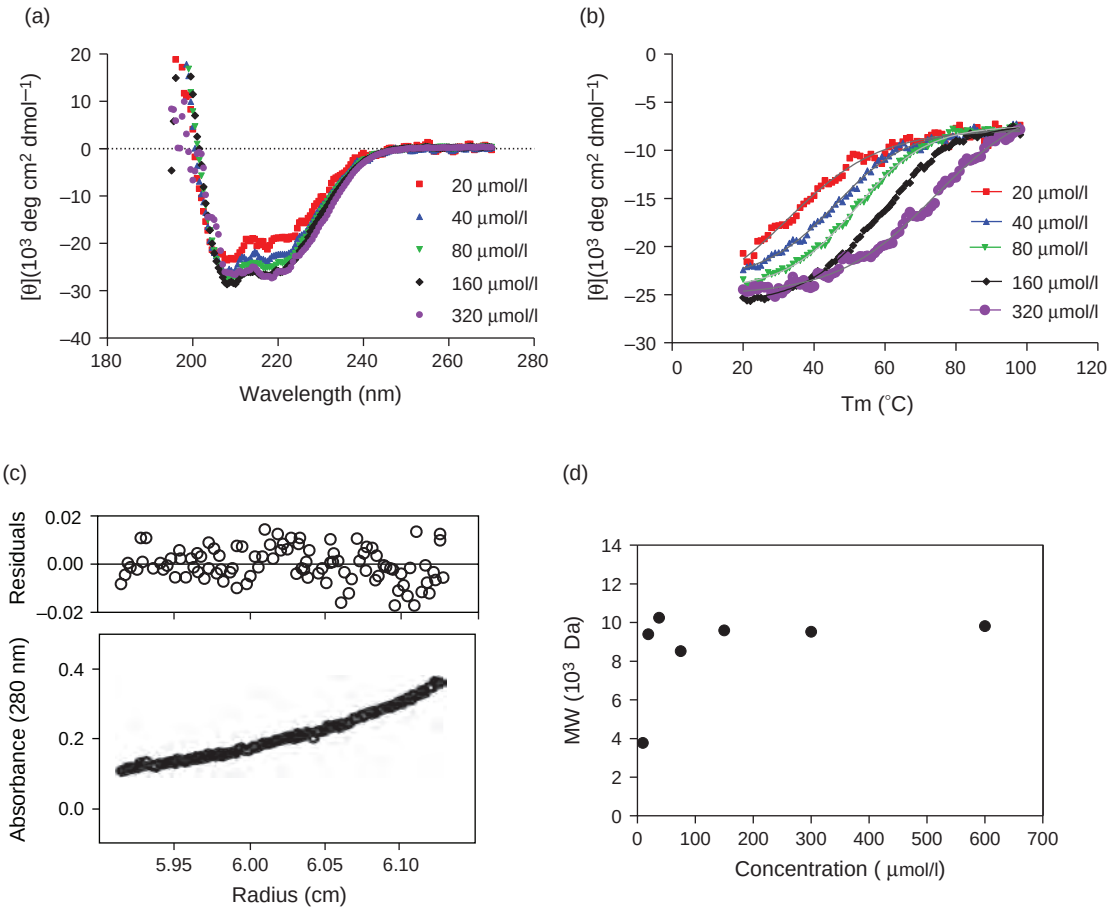

Fig. 2. Biophysical properties of HP23 in isolation. The α-helicity (a) and thermostability (b) of HP23 at different concentrations in PBS were determined using CD spectroscopy. (c) Molecular mass of HP23 was determined using sedimentation equilibrium ultracentrifugation at a concentration of 150 μmol/l in PBS (pH 7.0) at a rotor speed of 32 000 rpm at 20°C. The data are fitted to a single ideal species model and yield a weight-averaged molecular weight (MW) of 9598 Da. (d) The observed MW as a function of HP23 concentration.

binding of HP23 could be enhanced further. Circular dichroism spectroscopy was first applied to compare the α-helicity and thermal stability of HP23 and MT-SC22EK based 6-HBs in the presence of the NHR-derived peptide N36. Circular dichroism spectra showed that the HP23/N36 complex had a slightly increased helix content compared with the MT-SC22EK/N36 complex (Fig. 3a). The thermostability of each complex, defined as the midpoint of the thermal unfolding transition (T_m) value, was measured (Fig. 3b). Strikingly, the T_m value of the HP23/N36 complex reached 88.2°C, which indicated an increase of 10°C relative to the MT-SC22EK/N36 complex (78.1°C). The HP23-based 6-HB showed the most stable binding activity compared with a panel of well known control peptides and several M-T hook-modified peptides (Table 1).

We further determined the thermodynamic profiles of the molecular interaction between the inhibitors (HP23 or MT-SC22EK) and N36 using ITC technology. The released or absorbed heat during the interaction allowed an accurate measurement of the binding constant (K), reaction stoichiometry (N), enthalpy (ΔH) and entropy (ΔS). Figure 3c,d shows that HP23 and MT-SC22EK interacted with N36 in a typical enthalpy-driven reaction in which a large amount of heat was released. In comparison, the K value of HP23 increased approximately four-fold (from 3.3×10^6 to 1.3×10^7 mol/l).

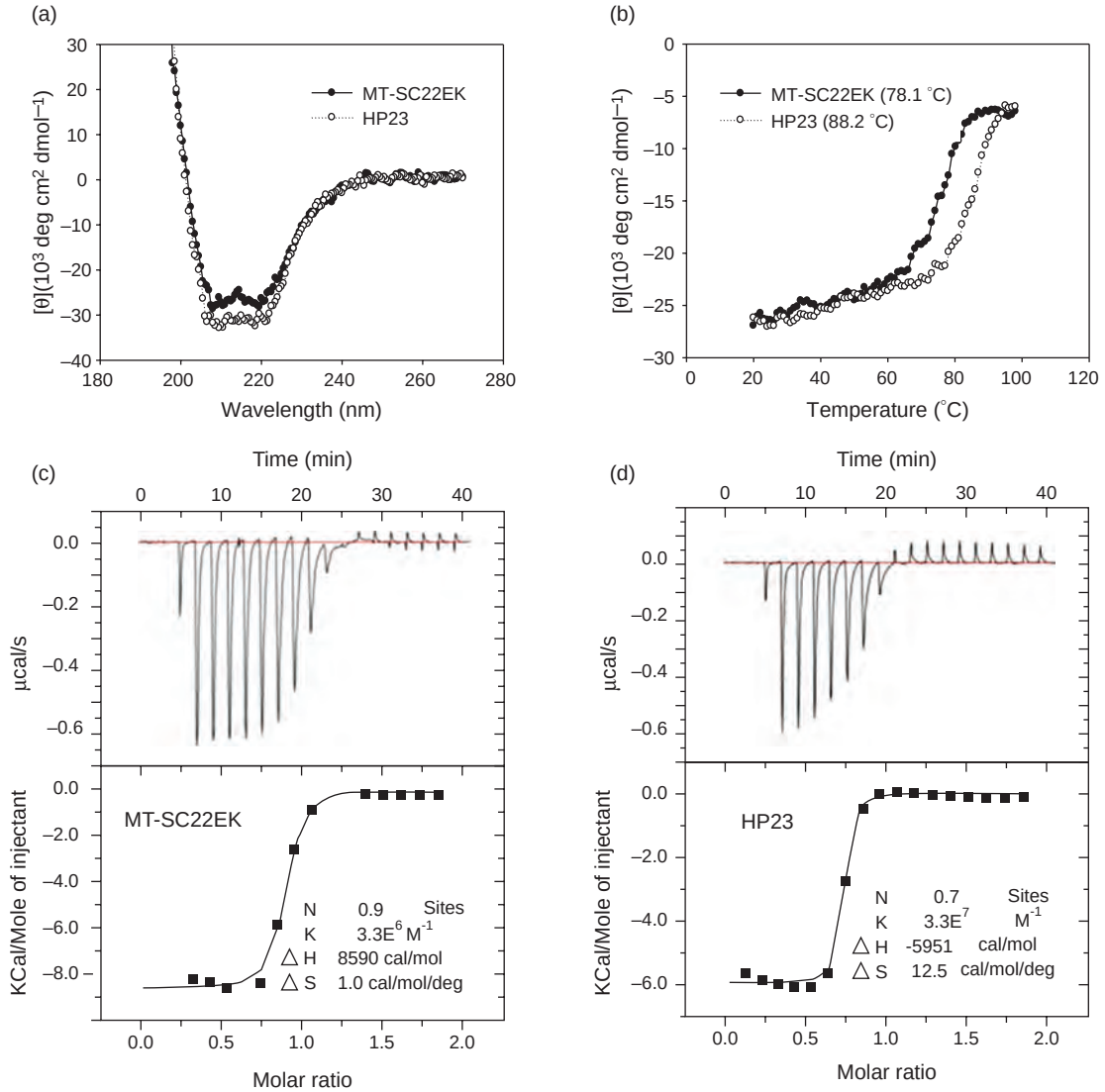

Fig. 3. Binding stability of HP23 and MT-SC22EK to the N-terminal heptad repeat derived peptide N36. The α-helicity (a) and thermostability (b) of 6-HB formed by HP23 or MT-SC22EK and N36 were determined using CD spectroscopy. Final concentration of each peptide in PBS is 10 μmol/l. The thermodynamic profiles of the molecular interactions between HP23 (c) or MT-SC22EK (d) and N36 were determined using ITC technology. The upper panels show the titration traces, and the lower panels show the binding affinity when the N36 solution was injected into an HP23 or MT-SC22EK solution.

Table 1. Binding stability and anti-HIV activity of HP23 and control peptides.[a]

Inhibitor	Length (a.a.)	CD data		IC_{50} (nmol/l)	
		Helix (%)	T_m (oC)	Virus entry	Replication
T20	36	NA	NA	70.3 ± 5.8	51.5 ± 2.7
C34	34	82.4	64.1	2.1 ± 0.1	1.1 ± 0.2
SFT	36	81.9	72.1	2.3 ± 0.2	1.4 ± 0.1
CP32M	32	79.8	81.3	1.7 ± 0.1	0.8 ± 0.1
T1249	39	26.8	57	1.6 ± 0.2	1.3 ± 0.1
T2635	38	81	82.1	0.9 ± 0.1	0.5 ± 0.1
SC29EK	29	79.2	67.1	1.9 ± 0.3	1.0 ± 0.1
SC22EK	22	79	64.1	64.2 ± 5.1	84.2 ± 4.7
MT-C34	36	83.2	75	0.7 ± 0.1	0.3 ± 0.0
MT-SFT	37	83.2	80.2	0.9 ± 0.1	0.4 ± 0.0
MT-SC29EK	31	88.6	77.2	0.8 ± 0.1	0.2 ± 0.0
MT-SC22EK	24	85.2	78.2	1.9 ± 0.1	1.2 ± 0.1
HP23	23	89.4	88.2	0.4 ± 0.0	0.1 ± 0.0

a.a, the number of amino acids for the peptides; CD, circular dichroism; NA, not applicable.
[a]The data for the M-T hook-modified peptides are highlighted in bold. The IC_{50} data were derived from the results of at least three independent experiments and expressed as means ± SD.

HP23 potently inhibited HIV-1 mediated cell fusion, entry and infection

We determined the antiviral potency of HP23 based on the biophysical data. The inhibitory activity of HP23 and MT-SC22EK on HIV-1_{NL4-3} Env-mediated cell–cell fusion was compared. Figure S1A, http://links.lww.com/QAD/A593 shows that HP23 and MT-SC22EK had IC_{50} values of 0.5 and 2.8 nmol/l, respectively, which indicated a 5.6-fold increase for HP23. The inhibition of HP23 and MT-SC22EK on HIV-1 entry was determined using a single-cycle infection assay (Fig. S1B, http://links.lww.com/QAD/A593). HP23 and MT-SC22EK inhibited HIV-1_{NL4-3} pseudovirus with IC_{50} values of 0.4 and 1.9 nmol/l, respectively, which indicated a 4.8-fold increase. We compared the actions of HP23 and MT-SC22EK on the replication of wild-type HIV-1_{NL4-3}. Figure S1C, http://links.lww.com/QAD/A593 shows that HP23 had an IC_{50} of 0.1 mol/l, whereas MT-SC22EK had an IC_{50} of 1.2 nmol/l, which indicated a 12-fold increase. In parallel, we tested a large panel of control peptides, such as T20, C34, SFT, CP32M, T1249, T2635 and SC29EK, and multiple M-T hook-modified peptides, such as MT-C34, MT-SFT and MT-SC29EK (Table 1). Promisingly, HP23 was the most potent inhibitor of HIV-1 entry and infection.

HP23 is a potent inhibitor against diverse HIV-1 subtypes

HIV-1 evolves with great genetic diversity, and it can be classified into diverse subtypes, which raises concerns about peptide fusion inhibitors that target the viral Env protein. Therefore, we constructed a large panel of HIV-1 pseudoviruses using Envs derived from primary subtypes A, B and C viruses that represent the majority of HIV-1 infections worldwide and the recombinant forms, CRF01_BC and CRF01_AE, and subtype B′ viruses that currently dominate the epidemic in China. The susceptibility of HP23 compared with MT-SC22EK and C34 against diverse HIV-1 subtypes was evaluated in single-cycle infection assays, and the results are presented in Table S1, http://links.lww.com/QAD/A593. Significantly, HP23 potently inhibited different pseudoviruses with an average IC_{50} of 1.3 nmol/l, whereas MT-SC22EK and C34 had average IC_{50} values of 6.3 and 3.9 nmol/l, respectively.

HP23 is a potent inhibitor of T20 and MT-SC22EK resistant HIV-1 mutants

We previously demonstrated that M-T hook-modified peptides, including MT-C34 [18], MT-SFT [25], MT-SC29EK [24] and MT-SC22EK [19], possessed highly improved activity against T20-resistant HIV-1 variants that carry single or double responsible mutations. However, some mutations still conferred high-level resistance, such as N43K, D36S/V38M and I37T/N43K. We expected that HP23 would react better against resistant HIV-1 mutants based on its high binding and antiviral activities. Therefore, a T20-resistant pseudovirus panel was used to compare HP23 with MT-SC22EK (Table 2). Consistently, HP23 had a higher potency than its template for the inhibition of all HIV-1 variants. More promisingly, HP23 efficiently inhibited variants that were resistant to MT-SC22EK, such as N43K, D36S/V38M and I37T/N43K.

Next, we compared the binding affinity of HP23 and MT-SC22EK to NHR mutants, which may help gain insights into the mechanism of HP23. A panel of N36-based peptides that carried a single (I37T, V38A, Q40H, N43K) or double (I37T/N43K and V38A/N42T) NHR mutation were applied in circular dichroism analyses. Figure S2, http://links.lww.com/QAD/A593 demonstrates that HP23 consistently enhanced binding stability compared with MT-SC22EK.

Table 2. Inhibitory activity of HP23 against T20 and MT-SC22EK resistant HIV-1 variants.[a]

	T20		MT-SC22EK		HP23	
HIV-1_{NL4-3}	IC_{50}	*n*-fold	IC_{50}	*n*-fold	IC_{50}	*n*-fold
WT	70.8 ± 11.8	1 (8.9)	1.5 ± 0.2	1	0.4 ± 0.0	1
D36G	8.0 ± 0.9	0.1 (1)	1.7 ± 0.1	1.1	0.6 ± 0.0	1.5
I37T	443.3 ± 58.6	6.3 (55.4)	2.4 ± 0.1	1.6	0.7 ± 0.0	1.8
V38A	1073.0 ± 56.4	15.2 (134.1)	1.1 ± 0.2	0.7	0.4 ± 0.0	1
V38M	383.4 ± 32.6	5.4 (47.9)	1.5 ± 0.1	1	0.6 ± 0.0	1.5
Q40H	1327.2 ± 127.5	18.8 (165.9)	1.6 ± 0.3	1.1	0.5 ± 0.0	1.3
N43K	316.9 ± 51.3	4.5 (39.6)	12.8 ± 2.4	8.5	0.5 ± 0.0	1.3
D36S/V38M	235.6 ± 21.0	3.3 (29.5)	8.6 ± 1.1	5.7	0.6 ± 0.0	1.5
I37T/N43K	>2250	>31.8 (281.3)	27.3 ± 2.2	18.2	0.7 ± 0.1	1.8
V38A/N42T	>2250	>31.8 (281.3)	1.8 ± 0.2	1.2	0.3 ± 0.0	0.8

[a]The IC_{50} data were derived from the results of three independent experiments and expressed as means ± SD. *n*-fold values are relative to the IC_{50} of the wild-type (WT) virus, while shown in parentheses for T20 are based on the D36G as a reference.

HP23 displays a high genetic barrier to the development of resistance

We recently found that M-T hook structure modified HIV-1 fusion inhibitors (MT-C34, MT-SFT, MT-SC29EK and MT-SC22EK) have higher genetic barriers than unmodified peptides (C34, SFT, SC29EK and SC22EK) to the development of resistance [24,25]. In our previous studies, HP23 was also included in the in-vitro selection of HIV-1 that was resistant to the inhibitors. Similar to the M-T hook-modified peptides, virus escape from inhibition by HP23 was much more difficult than escape from the unmodified peptides. Specifically, we could not successfully induce HP23-resistant HIV-1 variants after 25 generations of virus passages over 7 months (Fig. S3, http://links.lww.com/QAD/A593). Therefore, HP23 is a highly potent HIV-1 fusion inhibitor with a high genetic barrier to the development of drug resistance.

Discussion

The present study demonstrated the prominent features of HP23. It is a helical, trimeric short-peptide inhibitor that targets the conserved gp41 pocket. HP23 binds to the NHR target with a high affinity, and it displays the most potent anti-HIV activity among a panel of control CHR peptides. HP23 possesses high potency against diverse HIV-1 subtypes and T20-resistant mutants, and it displays a high genetic barrier to drug resistance. These features make HP23 an ideal candidate for further development for clinical use.

The crystal structure reveals that the gp41 pocket is nearly 16-Å long, nearly 7-Å wide and 5–6-Å deep, and it is formed by a cluster of 11 residues (Leu^{54}, Leu^{55}, Leu^{57}, Thr^{58}, Val^{59}, Trp^{60}, Gly^{61}, Ile^{62}, Lys^{63}, Leu^{65} and Gln^{66}) in the NHR coiled-coil. Three residues (Trp^{117}, Trp^{120} and Ile^{124}) from the PBD of the CHR helix are inserted into the pocket to cause extensive hydrophobic interactions [3–5]. The deep gp41 pocket has been extensively explored as a drug target, but small molecule-based and short peptide-based inhibitors directed to the pocket usually have low antiviral activity. Therefore, no compounds are available for clinical development [12,26–28]. The C34-based peptides, such as SFT, SC35EK and T2635, usually inherit a longer sequence that contains both PBD and NHR-binding domains [13,15,29]. A truncated PBD has been explored as a short-peptide inhibitor to specifically target the pocket region, but unfortunately, these truncations yield compounds with high μmol/l potency [14,30]. We recently demonstrated that the M-T hook structure of CHR peptides specifically targets the NHR pocket in which the residue Thr116 redirects the peptide chain to position Met115 above the left side of the pocket, and the side chain of Met115 caps the pocket to stabilize the PBD–pocket interaction [17,18]. On the basis of the M-T hook strategy, we successfully created the short-peptide MT-SC22EK, which primarily binds to the pocket region and exhibits anti-HIV activity comparable to C34-based large inhibitors [19]. Here, we successfully engineered MT-SC22EK into HP23, in which two C-terminal residues of MT-SC22EK that are not responsible for pocket-binding were deleted, and three middle residues that mediate the intra-helical and inter-helical interactions were intentionally changed. A glutamic acid was incorporated into the N-terminus of the peptide to stabilize M-T hook binding. As expected, the engineered HP23 exhibited dramatically improved binding affinity and antiviral activity compared with its template. The helical and oligomeric state of HP23 may also facilitate the interaction of this inhibitor with the NHR target, which improves its potency against HIV-1 mediated cell fusion, entry and infection, similar to the helical, oligomeric C34-based fusion inhibitor T2635 [15].

T20-resistance has been largely mapped to substitutions in the amino acid 36–45 within the inhibitor-binding site on the NHR helix [9–11,31,32]. We previously generated a panel of HIV-1 variants that carried single or double mutations frequently emerged in T20-treated patients and during in-vitro escape selection [23]. These hotspot mutations render the virus with a high-level

resistance to T20 that lacks the pocket-binding residues and mediate cross-resistance to the PBD sequence-containing CHR peptides (C34, SFT and SC29EK) [18,24,25], which poses a great challenge for the development of next-generation HIV-1 fusion inhibitors. On the basis of the mutational analysis and molecular docking, Eggink *et al*. [33] described four resistance mechanisms: reduced contact, steric obstruction, electrostatic repulsion and electrostatic attraction. We proposed several additional mechanisms, including hydrogen bond disruption and hydrophobic contact disruption, based on the structure of SFT and its resistant mutations [34]. Regardless of the complexity of resistance mechanism, our studies demonstrated that the M-T hook structure serves as a vital strategy to counter drug resistance [17–19,24,25]. M-T hook-modified peptides, such as MT-C34 [18], MT-SFT [25], MT-SC29EK [24] and MT-SC22EK [19], possess dramatically improved inhibitory activity against notorious HIV-1 mutants. Notably, viruses with N43K, D36S/V38M or I37T/N43K mutations display considerable resistance to M-T hook-mediated antiviral activity, but HP23 can overcome this problem (Table 2).

An ideal next-generation HIV-1 fusion inhibitor must have potent activity against various HIV-1 subtypes and existing resistant mutants and possess a high genetic barrier to the development of resistance. Again, the M-T hook structure can confer this property on inhibitors. Direct comparisons of the resistance-developing profiles of several paired peptides (C34 and MT-C34, SFT and MT-SFT, SC29EK and MT-SC29EK, SC22EK and MT-SC22EK) demonstrated that the virus hardly escaped from inhibition by M-T hook-modified inhibitors, which sharply contrasts the unmodified peptides [24,25]. Promisingly, HP23 displayed a phenotype similar to M-T hook-modified inhibitors during in-vitro selection, which verifies its high genetic barrier to the development of drug resistance. The mechanisms of the potent activity of M-T hook structure-containing inhibitors, such as HP23, on known resistant HIV-1 mutants and the simultaneous display of high genetic barriers to resistance should be clarified. We think that HIV-1 cannot tolerate any induced mutations in the pocket residues that are extremely conserved during virus evolution. Also, the high binding activity may be a key factor to prevent viral escape by binding site mutations. The selection of viral escape and the mapping of the responsible mutations would help to answer these questions, which are priorities in our research pipelines.

In conclusion, HP23 has prominent advantages over many other peptide-based HIV-1 fusion inhibitors, including the short sequence, stable structure, high binding affinity, potent antiviral activity and improved genetic barrier to resistance. It is highly promising to be developed for clinical use and as a critical tool to explore the mechanisms of HIV-1 fusion and inhibition.

Acknowledgements

We thank Xiaoxia Yu and Zheng Wang at the Institute of Biophysics, Chinese Academy of Sciences for technical support for sedimentation equilibrium centrifugation. This work was supported by grants from the National Science Foundation of China (81473255, 81025009, 81271830) and the National 973 Program of China (2010CB530100). The funding agencies had no role in the study design, data collection and analysis, the decision to publish or preparation of the manuscript.

H.C., Z.Q., Y.S., L.Y. performed the experiments. H.C., Z.Q. and Y.H. analysed the data. Y.H. conceived and designed the study and drafted the manuscript. All authors read and approved the final manuscript.

Conflicts of interest

The authors have no commercial or other association that might pose a conflict of interest.

References

1. Eckert DM, Kim PS. **Mechanisms of viral membrane fusion and its inhibition.** *Annu Rev Biochem* 2001; **70**:777–810.
2. Colman PM, Lawrence MC. **The structural biology of type I viral membrane fusion.** *Nat Rev Mol Cell Biol* 2003; **4**:309–319.
3. Chan DC, Fass D, Berger JM, Kim PS. **Core structure of gp41 from the HIV envelope glycoprotein.** *Cell* 1997; **89**:263–273.
4. Tan K, Liu J, Wang J, Shen S, Lu M. **Atomic structure of a thermostable subdomain of HIV-1 gp41.** *Proc Natl Acad Sci U S A* 1997; **94**:12303–12308.
5. Weissenhorn W, Dessen A, Harrison SC, Skehel JJ, Wiley DC. **Atomic structure of the ectodomain from HIV-1 gp41.** *Nature* 1997; **387**:426–430.
6. Chan DC, Chutkowski CT, Kim PS. **Evidence that a prominent cavity in the coiled coil of HIV type 1 gp41 is an attractive drug target.** *Proc Natl Acad Sci U S A* 1998; **95**:15613–15617.
7. Chan DC, Kim PS. **HIV entry and its inhibition.** *Cell* 1998; **93**:681–684.
8. Weng Y, Weiss CD. **Mutational analysis of residues in the coiled-coil domain of human immunodeficiency virus type 1 transmembrane protein gp41.** *J Virol* 1998; **72**:9676–9682.
9. Rimsky LT, Shugars DC, Matthews TJ. **Determinants of human immunodeficiency virus type 1 resistance to gp41-derived inhibitory peptides.** *J Virol* 1998; **72**:986–993.
10. Baldwin CE, Sanders RW, Deng Y, Jurriaans S, Lange JM, Lu M, *et al*. **Emergence of a drug-dependent human immunodeficiency virus type 1 variant during therapy with the T20 fusion inhibitor.** *J Virol* 2004; **78**:12428–12437.
11. Greenberg ML, Cammack N. **Resistance to enfuvirtide, the first HIV fusion inhibitor.** *J Antimicrob Chemother* 2004; **54**: 333–340.
12. Berkhout B, Eggink D, Sanders RW. **Is there a future for antiviral fusion inhibitors?** *Curr Opin Virol* 2012; **2**:50–59.
13. He Y, Xiao Y, Song H, Liang Q, Ju D, Chen X, *et al*. **Design and evaluation of sifuvirtide, a novel HIV-1 fusion inhibitor.** *J Biol Chem* 2008; **283**:11126–11134.
14. Naito T, Izumi K, Kodama E, Sakagami Y, Kajiwara K, Nishikawa H, *et al*. **SC29EK, a peptide fusion inhibitor with enhanced alpha-helicity, inhibits replication of human immunodeficiency virus type 1 mutants resistant to enfuvirtide.** *Antimicrob Agents Chemother* 2009; **53**:1013–1018.
15. Dwyer JJ, Wilson KL, Davison DK, Freel SA, Seedorff JE, Wring SA, *et al*. **Design of helical, oligomeric HIV-1 fusion inhibitor peptides with potent activity against enfuvirtide-resistant virus.** *Proc Natl Acad Sci U S A* 2007; **104**:12772–12777.

16. Liu Z, Shan M, Li L, Lu L, Meng S, Chen C, *et al*. **In vitro selection and characterization of HIV-1 variants with increased resistance to sifuvirtide, a novel HIV-1 fusion inhibitor.** *J Biol Chem* 2011; **286**:3277–3287.
17. Chong H, Yao X, Qiu Z, Qin B, Han R, Waltersperger S, *et al*. **Discovery of critical residues for viral entry and inhibition through structural insight of HIV-1 fusion inhibitor CP621-652.** *J Biol Chem* 2012; **287**:20281–20289.
18. Chong H, Yao X, Sun J, Qiu Z, Zhang M, Waltersperger S, *et al*. **The M-T hook structure is critical for design of HIV-1 fusion inhibitors.** *J Biol Chem* 2012; **287**:34558–34568.
19. Chong H, Yao X, Qiu Z, Sun J, Zhang M, Waltersperger S, *et al*. **Short-peptide fusion inhibitors with high potency against wild-type and enfuvirtide-resistant HIV-1.** *FASEB J* 2013; **27**:1203–1213.
20. Gill SC, von Hippel PH. **Calculation of protein extinction coefficients from amino acid sequence data.** *Anal Biochem* 1989; **182**:319–326.
21. He Y, Liu S, Li J, Lu H, Qi Z, Liu Z, *et al*. **Conserved salt bridge between the N- and C-terminal heptad repeat regions of the human immunodeficiency virus type 1 gp41 core structure is critical for virus entry and inhibition.** *J Virol* 2008; **82**:11129–11139.
22. He Y, Cheng J, Lu H, Li J, Hu J, Qi Z, *et al*. **Potent HIV fusion inhibitors against Enfuvirtide-resistant HIV-1 strains.** *Proc Natl Acad Sci U S A* 2008; **105**:16332–16337.
23. Chong H, Yao X, Zhang C, Cai L, Cui S, Wang Y, *et al*. **Biophysical property and broad anti-HIV activity of albuvirtide, a 3-maleimimidopropionic acid-modified peptide fusion inhibitor.** *PLoS One* 2012; **7**:e32599.
24. Chong H, Qiu Z, Sun J, Qiao Y, Li X, He Y. **Two M-T hook residues greatly improve the antiviral activity and resistance profile of the HIV-1 fusion inhibitor SC29EK.** *Retrovirology* 2014; **11**:40.
25. Chong H, Yao X, Qiu Z, Sun J, Qiao Y, Zhang M, *et al*. **The M-T hook structure increases the potency of HIV-1 fusion inhibitor sifuvirtide and overcomes drug resistance.** *J Antimicrob Chemother* 2014; **69**:2759–2769.
26. Eggink D, Berkhout B, Sanders RW. **Inhibition of HIV-1 by fusion inhibitors.** *Curr Pharm Des* 2010; **16**:3716–3728.
27. Steffen I, Pohlmann S. **Peptide-based inhibitors of the HIV envelope protein and other class I viral fusion proteins.** *Curr Pharm Des* 2010; **16**:1143–1158.
28. He Y. **Synthesized peptide inhibitors of HIV-1 gp41-dependent membrane fusion.** *Curr Pharm Des* 2013; **19**:1800–1809.
29. Otaka A, Nakamura M, Nameki D, Kodama E, Uchiyama S, Nakamura S, *et al*. **Remodeling of gp41-C34 peptide leads to highly effective inhibitors of the fusion of HIV-1 with target cells.** *Angew Chem Int Ed Engl* 2002; **41**:2937–2940.
30. Eckert DM, Malashkevich VN, Hong LH, Carr PA, Kim PS. **Inhibiting HIV-1 entry: discovery of D-peptide inhibitors that target the gp41 coiled-coil pocket.** *Cell* 1999; **99**:103–115.
31. Sista PR, Melby T, Davison D, Jin L, Mosier S, Mink M, *et al*. **Characterization of determinants of genotypic and phenotypic resistance to enfuvirtide in baseline and on-treatment HIV-1 isolates.** *AIDS* 2004; **18**:1787–1794.
32. Ashkenazi A, Wexler-Cohen Y, Shai Y. **Multifaceted action of Fuzeon as virus-cell membrane fusion inhibitor.** *Biochim Biophys Acta* 2011; **1808**:2352–2358.
33. Eggink D, Langedijk JP, Bonvin AM, Deng Y, Lu M, Berkhout B, *et al*. **Detailed mechanistic insights into HIV-1 sensitivity to three generations of fusion inhibitors.** *J Biol Chem* 2009; **284**:26941–26950.
34. Yao X, Chong H, Zhang C, Waltersperger S, Wang M, Cui S, *et al*. **Broad antiviral activity and crystal structure of HIV-1 fusion inhibitor sifuvirtide.** *J Biol Chem* 2012; **287**:6788–6796.